

# Cu Ion Ink for a Flexible Substrate and Highly Conductive Patterning by Intensive Pulsed Light Sintering

Byung-Yong Wang,<sup>†,‡</sup> Tae-Hee Yoo,<sup>†</sup> Yong-Won Song,<sup>†</sup> Dae-Soon Lim,<sup>‡</sup> and Young-Jei Oh<sup>\*,†,§</sup>

<sup>†</sup>Future Convergence Technology Research Division, Korea Institute of Science and Technology, Seoul 136-791, Republic of Korea

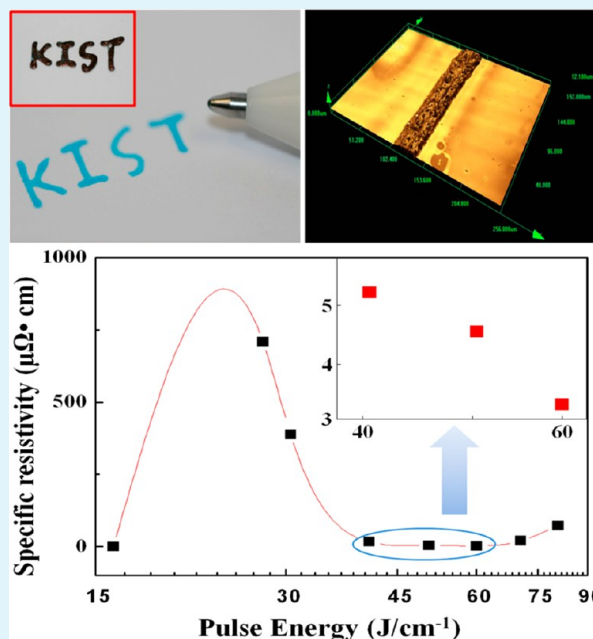
<sup>‡</sup>Division of Materials Science and Engineering, Korea University, Seoul 136-701, Republic of Korea

<sup>§</sup>Department of Nano Material Science and Engineering, University of Science and Technology, Daejeon 305-333, Republic of Korea

## S Supporting Information

**ABSTRACT:** Direct printing techniques that utilize nanoparticles to mitigate environmental pollution and reduce the processing time of the routing and formation of electrodes have received much attention lately. In particular, copper (Cu) nanoink using Cu nanoparticles offers high conductivity and can be prepared at low cost. However, it is difficult to produce homogeneous nanoparticles and ensure good dispersion within the ink. Moreover, Cu particles require a sintering process over an extended time at a high temperature due to high melting temperature of Cu. During this process, the nanoparticles oxidize quickly in air. To address these problems, the authors developed a Cu ion ink that is free of Cu particles or any other impurities. It consequently does not require separate dispersion stability. In addition, the developed ink is environmentally friendly and can be sintered even at low temperatures. The Cu ion ink was sintered on a flexible substrate using intense pulsed light (IPL), which facilitates large-area, high-speed calcination at room temperature and at atmospheric pressures. As the applied light energy increases, the Cu<sub>2</sub>O phase diminishes, leaving only the Cu phase. This is attributed to the influence of formic acid (HCOOH) on the Cu ion ink. Only the Cu phase was observed above 40 J cm<sup>-2</sup>. The Cu-patterned film after sintering showed outstanding electrical resistivity in a range of 3.21–5.27 μΩ·cm at an IPL energy of 40–60 J cm<sup>-2</sup>. A spiral-type micropattern with a line width of 160 μm on a PI substrate was formed without line bulges or coffee ring effects. The electrical resistivity was 5.27 μΩ·cm at an energy level of 40.6 J cm<sup>-2</sup>.

**KEYWORDS:** Cu ion ink, flexible substrate, high electric conductivity, inkjet printing, rollerball pen, intensive pulsed light



## 1. INTRODUCTION

The printing process technique can be used for large area applications through a relatively simple process at low temperatures compared to existing general electronic printing processes, such as vapor deposition, photolithography, and sputtering. As such, it is environmentally friendly while also being inexpensive. In addition, it enables fabrication on flexible substrates, which is impossible with conventional processes, and it can be applied in numerous areas.<sup>1</sup> Furthermore, electronic printing techniques have become essential technology in the fields of flexible electronics and components, such as radio frequency identification (RFID), solar cells, displays, thin-film transistors, and printed circuit boards (PCBs).<sup>2–6</sup>

Among printed electronic techniques, inkjet printing is a contactless printing technique that allows highly selective patterning. Using this type of printing, micropatterning is

possible without damage to devices through contact and with little loss of materials. On the basis of these characteristics, it is also cost-effective.<sup>7</sup> However, the use of a metal powder ink is problematic, as the ink should be solvent based. It becomes difficult to control the solvent used in making the ink, and the metal powder, the size of the powder particles, and dispersion characteristics of the metal powder also become difficult to control.<sup>8–10</sup> Moreover, a solvent-based ink must have an optimal ink formulation in order to achieve patterns without a coffee ring effect. Heterogeneity can also arise after printing due to differences in the drying speed when a large area is coated. In particular, when metal powders are used, they must be

**Received:** December 27, 2012

**Accepted:** April 15, 2013

**Published:** April 15, 2013

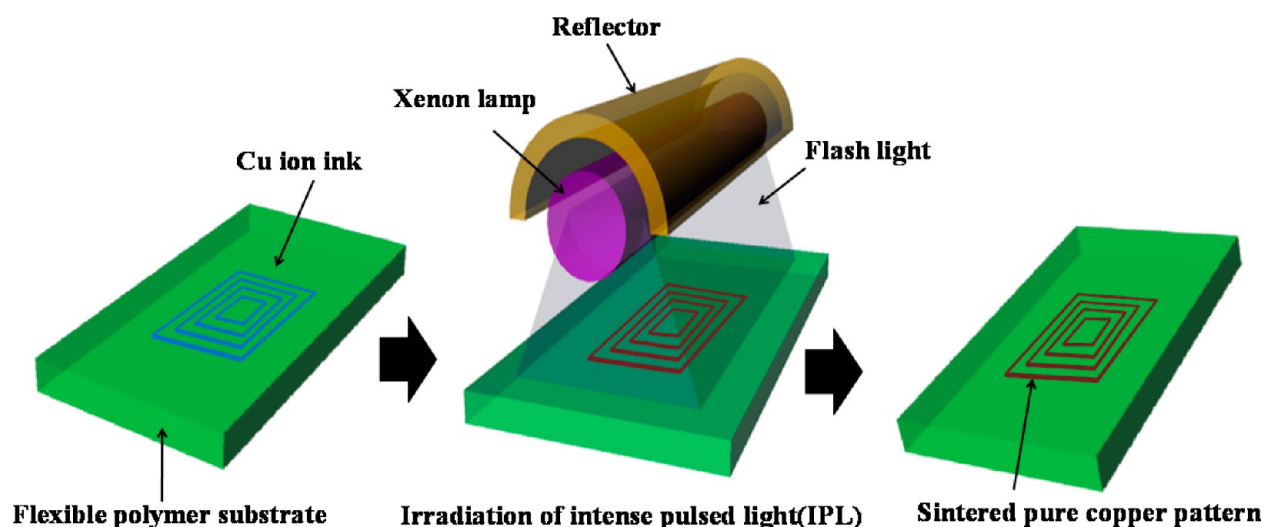


**Figure 1.** Schematic diagram of the patterning process by the ion ink using the IPL device.

thoroughly dispersed within the ink. However, to achieve this, a large amount of dispersants and other organic compounds must be added, which necessitates a calcination process at a high temperature. To address this issue, studies of how to manufacture copper (Cu) complex inks using electrolysis have been carried out.<sup>11</sup> However, electrolysis is a complicated process that is limited in terms of the ion concentration adjustment, with the resulting pattern thickness being very thin after drying and calcination.

Metallic substances with superb electronic conductivity are widely used as conduction line substances. Many studies have been carried out on materials such as platinum, silver, copper, and aluminum, which are known to have excellent electrical properties. Unlike aluminum and copper, other metals are costly. Aluminum, in particular, is currently the most widely used metal, and many studies have been performed using it. However, its electric conductivity is only 60% that of copper. Therefore, current research has focused on copper, which is inexpensive and offers excellent electrical properties.<sup>10,12</sup> However, the use of copper is limited, as its electrical properties are compromised because copper nanoparticles oxidize quickly in air.

In addition, to ensure an active flow of the electronic charge by the sintering of the Cu ink, sintering for an extended time at the high melting temperature of Cu nanoparticles is required. However, under these conditions, flexible substrates used for sintering can easily be damaged due to heat, negatively affecting the originally designed structure of the device and its operation. Therefore, the conventional thermal sintering method is not appropriate.

Thermal sintering,<sup>8</sup> laser sintering,<sup>13</sup> low-pressure argon plasma exposure,<sup>14</sup> and microwave radiation<sup>15</sup> are sintering processes typically used with Cu particles. However, existing methods are limited with regard to the types of substrates that can be used due to the high sintering temperatures and applicability to large areas. Cu, in particular, which oxidizes easily, must be sintered in an inert gas and a reducing gas atmosphere and therefore requires complicated sintering processes and equipment.<sup>10,16</sup>

To address these issues, the authors developed a Cu ion ink that is easy to fabricate, offers excellent oxidative stability, has no particles or other impurities, does not require dispersion

stability, is environmentally friendly, and can be fabricated at a low temperature. An intense pulsed light (IPL)<sup>17–19</sup> with a wavelength of 200 nm to 2  $\mu\text{m}$ , which allows large-area, high-speed sintering at room temperature and at atmospheric pressure without any limitation in terms of the type of substrates used, was irradiated very briefly on a sample patterned with ion ink instantaneously for calcination under room temperature conditions. Figure 1 shows a graphic representation of the IPL device.

## 2. EXPERIMENTAL SECTION

**2.1. Preparation of Cu Ion Ink.** To fabricate the Cu ion ink used in this study, 50 mL of DI water was poured into a beaker into which copper(II) hydroxide and  $\text{NH}_4\text{OH}$  were added. This was then agitated for 30 min. The liquid then turned bluish, and to this, formic acid ( $\text{HCOOH}$ , 99.5% purity; Sigma-Aldrich) and citric acid ( $\text{C}_6\text{H}_8\text{O}_7$ , 99.5% purity; Yakuri Chemical) were added as complexing agents for Cu ion reduction and stabilization. In this manner, metal ions were created. Because  $\text{NH}_4\text{OH}$  was used as a complexing agent for ions, Cu ions were naturally generated, even without other complexing agents. However, if the solubility of the Cu ions was low, they precipitated as a hydroxide ( $\text{Cu}(\text{OH})_2$ ) or an oxide ( $\text{Cu}_2\text{O}$  or  $\text{CuO}$ ). The fabricated Cu ion ink has a pH value of 8, and its color is a very dark indigo. Moreover, below a pH value of 8, it is difficult to form homogeneous patterns due to the low ion content, while above a pH value of 9, Cu compounds precipitated (Figure 1). This phenomenon is a result of the carboxyl group, and for this study, the pH and complexing agents added are the most important factors.<sup>20,21</sup> Finally, to achieve a level of viscosity and a degree of surface tension that enable jetting in an inkjet printer while eliminating the coffee ring effects phenomenon caused by solvent evaporation, 2-methoxyethanol (99.8% purity; Sigma-Aldrich) and ethylene glycol (99.5% purity; Junsei Chemical) were mixed at a ratio of 90:10, after which poly (*N*-vinylpyrrolidone) (PVP, MW = 40 000  $\text{g mol}^{-1}$ , Sigma-Aldrich) was added to fabricate the final Cu ion ink.

**2.2. Pattern Formation and Characterization.** To form Cu conductive patterns, actual handwriting with a rollerball pen and a SonoPlot GIX Desktop Microplotter offering inkjetting accuracy and patterning equipment movement accuracy were used, and the patterning was performed at a printing speed of 200  $\mu\text{m/s}$  with a 30  $\mu\text{m}$  nozzle tip.

PET (polyethylene terephthalate) and PI (Polyimide) films, which are used as flexible substrates for electronic components, were used during the patterning process. Also, the substrates show changes in the final patterning characteristics depending on the surface treatment. In this study, the substrates were rendered hydrophilic for patterning, for the substrate processing was carried out using nitrogen plasma

treatment. Surface processing involved  $N_2$  gas, 50 sccm at an output of 250 W for 40 s.

The fabricated pattern was sintered at room temperature in air using the IPL sintering method, and the characteristics of light energies were observed. The IPL system used in this study covered broad band emission ranging from 160 nm to  $2.5 \mu\text{m}$ ; the specimen size for sintering is  $10 \text{ cm} \times 2 \text{ cm}$ , and the pulsed light energy is  $0.3\text{--}102 \text{ J cm}^{-2}$ .

To compare the oxidation stability and crystallization of the IPL-treated Cu patterns, an X-ray diffraction analysis (XRD, Model Rint/Dmax 2500, Rigaku Co., Japan) with Cu  $K\alpha$  radiation with a wave  $\lambda$  of 0.154 nm was conducted. The microstructures and thicknesses of the patterns were observed by means of scanning electron microscopy (SEM; XL-30 EDAX, Philips, Netherlands), and the surface resistance was measured using a 4-point probe and by inkjet-printing with a size of  $1 \text{ cm} \times 1 \text{ cm}$  and a thickness of  $4 \pm 0.5 \mu\text{m}$ . Also, the measured thickness of the patterns was replaced with the surface resistance to calculate the electric resistivity. Finally, a  $2.5 \text{ cm} \times 2.5 \text{ cm}$  area was fabricated with Cu ion ink to evaluate the flexibility of the inkjet-printed Cu layer on a PI substrate. The flexibility test was performed on the basis of the method suggested by Park et al.<sup>22</sup>

### 3. RESULTS AND DISCUSSION

The evaluation of the solubility of the Cu ion ink based on the pH level (Figure 2) revealed that it is dark indigo at pH 8 and

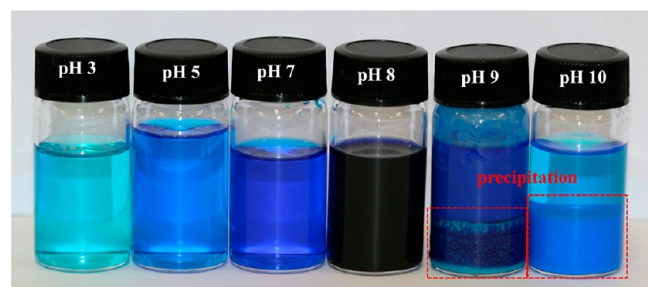


**Figure 2.** Color changes of the fabricated Cu ion ink as a function of pH.

light blue below pH 8 due to low Cu ion content. However, at pH 8 or higher, copper oxide ( $\text{Cu}_2\text{O}$  or  $\text{CuO}$ ) was precipitated. Moreover, the color of the ink changed from dark indigo to light blue, because the main precipitate during the initial reaction was  $\text{Cu}_2\text{O}$ , which then was gradually taken over by  $\text{CuO}$ . Preliminary testing revealed that, under pH 8, the Cu ion content was low, which makes it difficult to fabricate a homogeneous film through the clustering of ions as they undergo the processes of drying and sintering. The precipitation phenomenon at pH 8 or higher can be confirmed by a Pourbaix diagram. Cu ions are formed due to the presence of formic acid and citric acid. During this process, they are combined with a carboxyl group ( $\text{COOH}$ ) with the greatest degree of solubility. Therefore, if the carboxyl group exists at a low content level, the solubility will be low, which makes it impossible for Cu to be ionized. As a result, it is precipitated as an oxide or hydroxide.<sup>8,11</sup>

The ink fabricated at pH 8 went through Cu ion ink patterning based on the energy level applied at room temperature and atmospheric pressure by IPL, and its sintering characteristics and microstructure were observed. The Cu pattern was fabricated by inkjet printing using a PI substrate. Each sample was heat-treated under the energy conditions shown in Table 1 for a comparison of their characteristics.

**Table 1.** Total Energy Changes Based on the Pulse Conditions of IPL

sample	pulse width (ms)	gap between pulses (ms)	number of pulses (time)	total energy ( $\text{J cm}^{-2}$ )
A	1.5	12	20	16.5
B	1.5	12	40	27.6
C	1.5	30	17	30.5
D	1.5	30	23	40.6
E	1.5	30	30	50.5
F	1.5	30	36	60.0
G	1.5	30	40	70.5
H	1.5	30	46	80.7

Figure 3 shows SEM surface images of the Cu patterns in relation to the IPL heat treatment conditions. At the initial energy of  $16 \text{ J cm}^{-2}$ , the energy applied to the Cu patterns was low; the organic compounds used during the ink fabrication process were consequently not burned, and the Cu particles were covered with films of an organic compound. It was also confirmed that cracks formed easily. For this reason, the electrical resistance was not measured. Also, at  $30.5 \text{ J cm}^{-2}$ , the organic compounds did not combust completely, and the combustion of organic compounds inside the Cu films resulted in holes. The electrical resistivity at this point was  $388.3 \mu\Omega\text{-cm}$ . In this case, as well, the organic compounds were not completely burned, and some existed as Cu oxides (Figure 4), leading to high resistance levels. However, at  $40.6 \text{ J cm}^{-2}$ , the organic compounds combusted completely and were covered with small particles. It was also confirmed that bonds were created between the particles. It appears that Cu nucleation occurred upon the heat treatment, causing the Cu particles to grow. Because they have very close structures among themselves, the electrical resistivity was very low ( $4.62 \mu\Omega\text{-cm}$ ). Meanwhile, a surface with crater-like pores in a relatively homogeneous form was observed at  $50.5 \text{ J cm}^{-2}$ . These pores were created as a large volume of gases was released suddenly as the organic substances inside the Cu pattern burned readily in a very short period of time due to the high energy of the IPL instantly applied to the Cu pattern film. However, the micropores that formed on the Cu patterns are not clearly observable and exist as a film with a very high density of Cu, demonstrating excellent electrical resistivity at  $3.21 \mu\Omega\text{-cm}$ . Above  $70.5 \text{ J cm}^{-2}$ , due to the instantly applied high energy, bubbling arose on the surface of the Cu film, which created many pores, thus making the pattern uneven. The electrical resistivity at this time was  $20.63 \mu\Omega\text{-cm}$  due to the large number of pores and the surface heterogeneity. This is much lower than the electrical resistivity of  $45 \mu\Omega\text{-cm}$  recorded in a previous study<sup>23</sup> for low-temperature sintering under  $150 \text{ }^\circ\text{C}$  using a Cu nanoparticle ink, but its high energy at  $70.5 \text{ J cm}^{-2}$  led to the deformation of the substrate. Also, no change was observed in the adhesive strength test at  $40.6\text{--}60 \text{ J cm}^{-2}$ , but the resistance increased rapidly at  $70.7 \text{ J cm}^{-2}$  due to bubbling, which prevented the copper particles from coagulating (Supporting Information S3).

Figure 4 shows the XRD result of the printed Cu pattern as a result of the IPL light energy. The Cu phase and the  $\text{Cu}_2\text{O}$  phase (JCPDS 01-077-0199) were observed for the sample that underwent patterning before IPL sintering at room temperature and in air.

However, as the applied light energy increases, the  $\text{Cu}_2\text{O}$  phase diminishes, leaving the Cu phase only; this appears to be

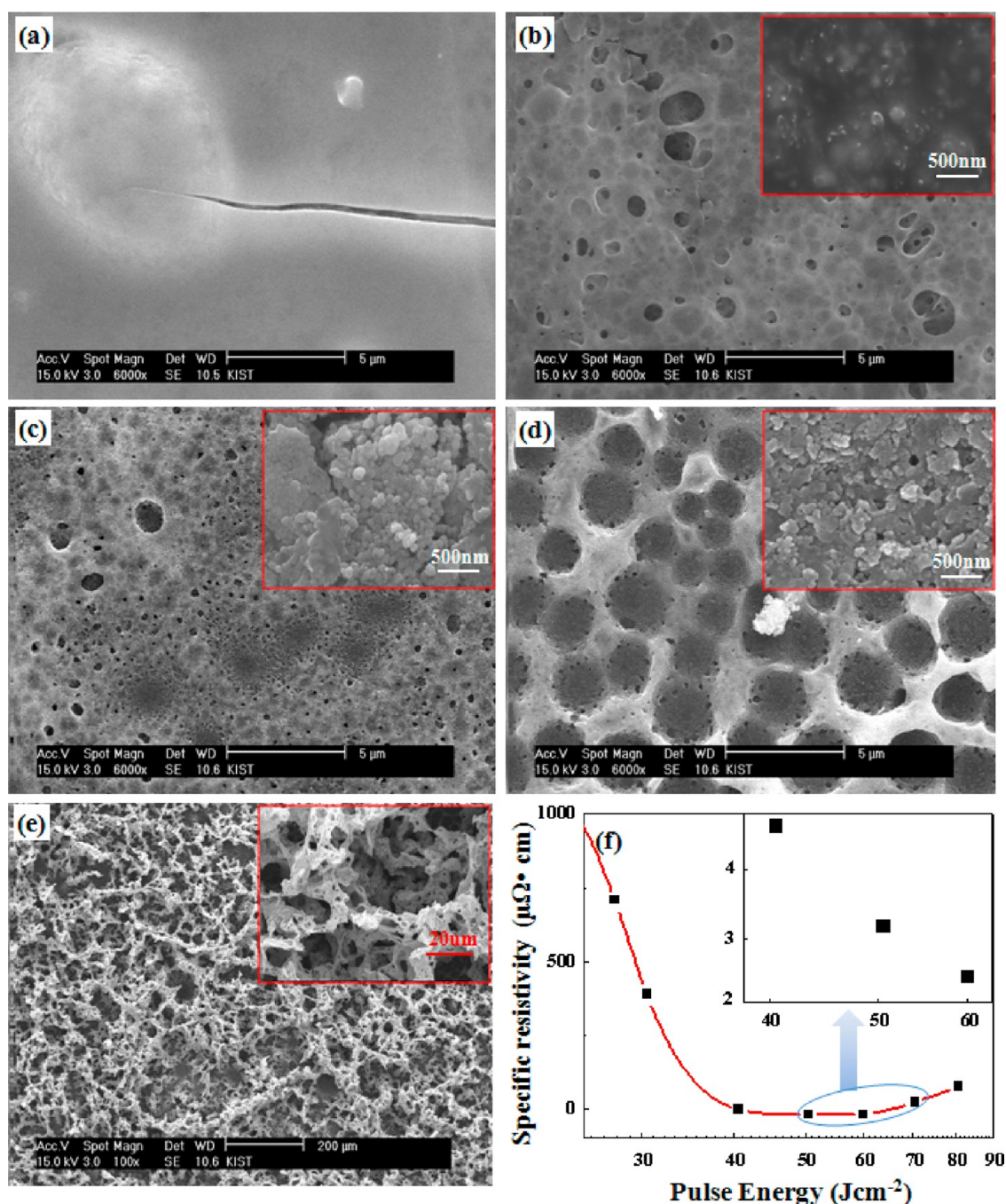
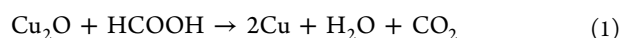


**Figure 3.** Microstructure and electric resistivity after the IPL treatment of the fabricated pattern with the Cu ion ink: (a)  $16.5 \text{ J cm}^{-2}$ , (b)  $30.5 \text{ J cm}^{-2}$ , (c)  $40.6 \text{ J cm}^{-2}$ , (d)  $50.5 \text{ J cm}^{-2}$ , (e)  $70.5 \text{ J cm}^{-2}$ , and (f) electric resistivity as a function of IPL energy (inset: high magnification image; pattern thickness:  $4 \pm 0.4 \mu\text{m}$ ).

due to the influence of formic acid,  $\text{HCOOH}$ , in the Cu ion ink. Formic acid starts to decompose at a low temperature ( $101^\circ\text{C}$ ) and is known to generate a large amount of  $\text{CO}$  gas during sintering. This can greatly enhance the reduction of the Cu ion ink; therefore, it is believed that decomposition of pulsed light energy starts at  $16.5 \text{ J cm}^{-2}$  and influences the reduction of the Cu ion ink via the emitted reducing gases.<sup>24,25</sup>



The heat energy applied to the Cu pattern film increases with greater IPL energy. When the heat energy increases, the organic substances that exist on the surface and inside of the Cu pattern

film are removed, leading to complete combustion of the formic acid and ammonia that existed in certain quantities inside the Cu patterns, thereby further maximizing the reducing nature of the Cu ion ink. In this case, only the Cu phase was observed beyond  $40 \text{ J cm}^{-2}$  with greater pulsed light energy.<sup>10,26,27</sup>

For flexible substrates, even if electrode patterns are well formed, the mechanical characteristics of the patterned flexible substrates, such as the bending radius, must be confirmed. Figure 5 shows the results of a bending test of a Cu ion pattern formed on a  $200 \mu\text{m}$ -thick polyimide (PI) substrate. Cracks formed on the Cu pattern as observed by SEM, and the flexibility of the Cu film was evaluated by measuring the

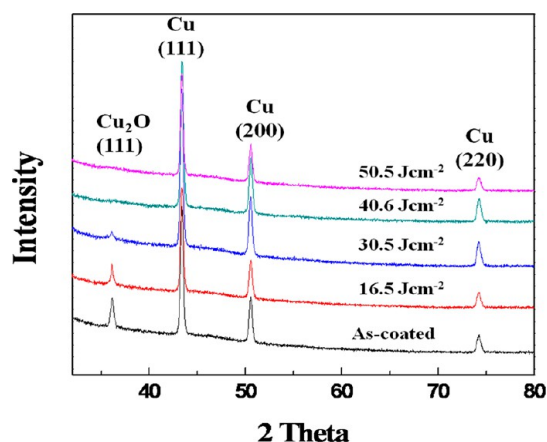


**Figure 4.** XRD patterns of the patterned Cu ion ink as a function of the IPL energy.

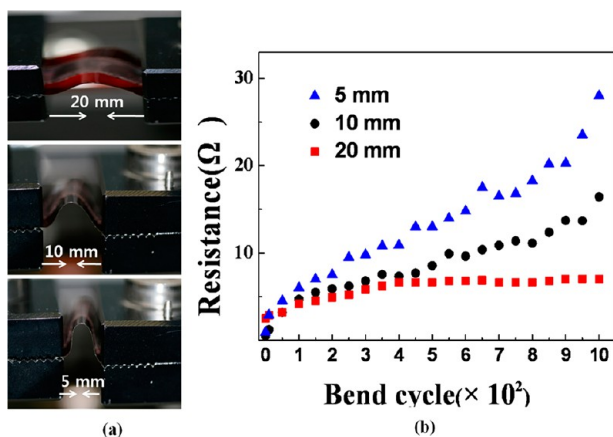


**Figure 5.** (a) Bending test images of 20 mm copper electrode arrays fabricated using Cu ion ink (top) and bent shapes with bend radii of 10 mm (middle) and 5 mm (bottom); (b) electrical resistance as a function of the bending cycle of the printed Cu electrodes according to the bend radius.

resistance change ratio. This experiment was carried out by reducing the curvature radius from 20 to 10 mm and then to 5 mm at 1 mm/s, as shown in Figure 5a. The initial resistance values were 0.9, 2.5, and 0.5  $\Omega$ . The experimental results (Figure 5b) show that, when the curvature ratio of the substrate was set at 20 mm, no major change in the resistance occurred, whereas at 10 mm and 5 mm, the resistance increased gradually and then started showing dramatic resistance changes over 100

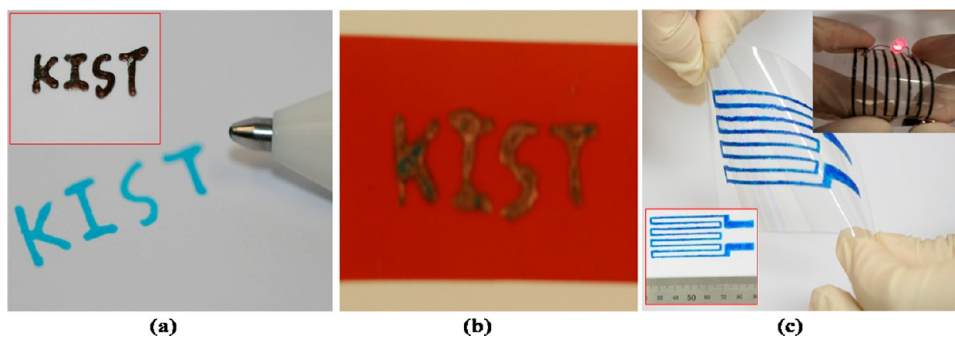
cycles. When it was reduced to 20 mm, cracks formed in a uniform manner on the bent side. As the curvature radius of the Cu pattern became narrower, cracks occurred readily not only on the bent side but also on the entire surface (Supporting Information S4).

Figure 6 shows printed samples on PET and PI substrates using a roller-ball pen. The pen used here had a ball diameter of 250  $\mu\text{m}$ . As shown in Figure 6a, showing a PET substrate, and Figure 6b, showing a PI substrate, a ballpoint pen can be used to write on the flexible substrates smoothly. Also, as shown in Figure 6c, simple electrode patterns can be created on a PET substrate without using currently existing printing equipment. This confirms that Cu patterns can be created without deformation of the substrates and patterns even after an IPL heat treatment (inset). Also, regarding the electrical properties during this process, the line resistance values of (a), (b), and (c) were low at 0.3, 0.2, and 0.6  $\Omega$ , respectively, in relation to the thickness of the patterns. Although there have been few studies on pattern formation using roller-ball pens, this method is expected to have diverse applications in the future to form conductive films easily with a simple printing process on various substrates.

Figure 7 shows the patterning results using the SonoPlot GIX Desktop Microplotter. Phenomena related to fluid instability, in this case line bulges or coffee ring effects, were completely eliminated by optimizing the inkjetting conditions and through a plasma treatment of the substrate. As a result, a spiral-type micropattern with a line width of 81  $\mu\text{m}$  could be created (Supporting Information S1). For the Cu conductive line printed on the PI substrate, it was confirmed that the homogeneous patterning of the Cu ion ink was achieved without stoppage or dispersion owing to the plasma treatment on the substrates. The result of IPL sintering at 40.6  $\text{J cm}^{-2}$  (Figure 7b,c) showed that a homogeneous conductive line was formed without line bulges or coffee ring effects. Also, for the reasons previously explained, a conductive line with a high copper density was formed. The electrical resistivity was 4.62  $\mu\Omega\text{-cm}$ , demonstrating superior electrical properties.

#### 4. CONCLUSIONS

In this study, Cu ion ink that offers excellent ion complex stability and dispersion stability was fabricated a simple solution process. This study has great academic significance, as a Cu ion ink with excellent electrical properties was fabricated after reducing the reaction through additives rather than through an electrolysis method. The Cu ion concentration could be adjusted on the basis of the pH, and highly concentrated Cu



**Figure 6.** Patterns of the ion ink printed using a roller-ball pen: (a) PET substrate (inset: IPL treated), (b) PI substrate (IPL treated), and (c) PET substrate (inset, upper right: IPL treated).

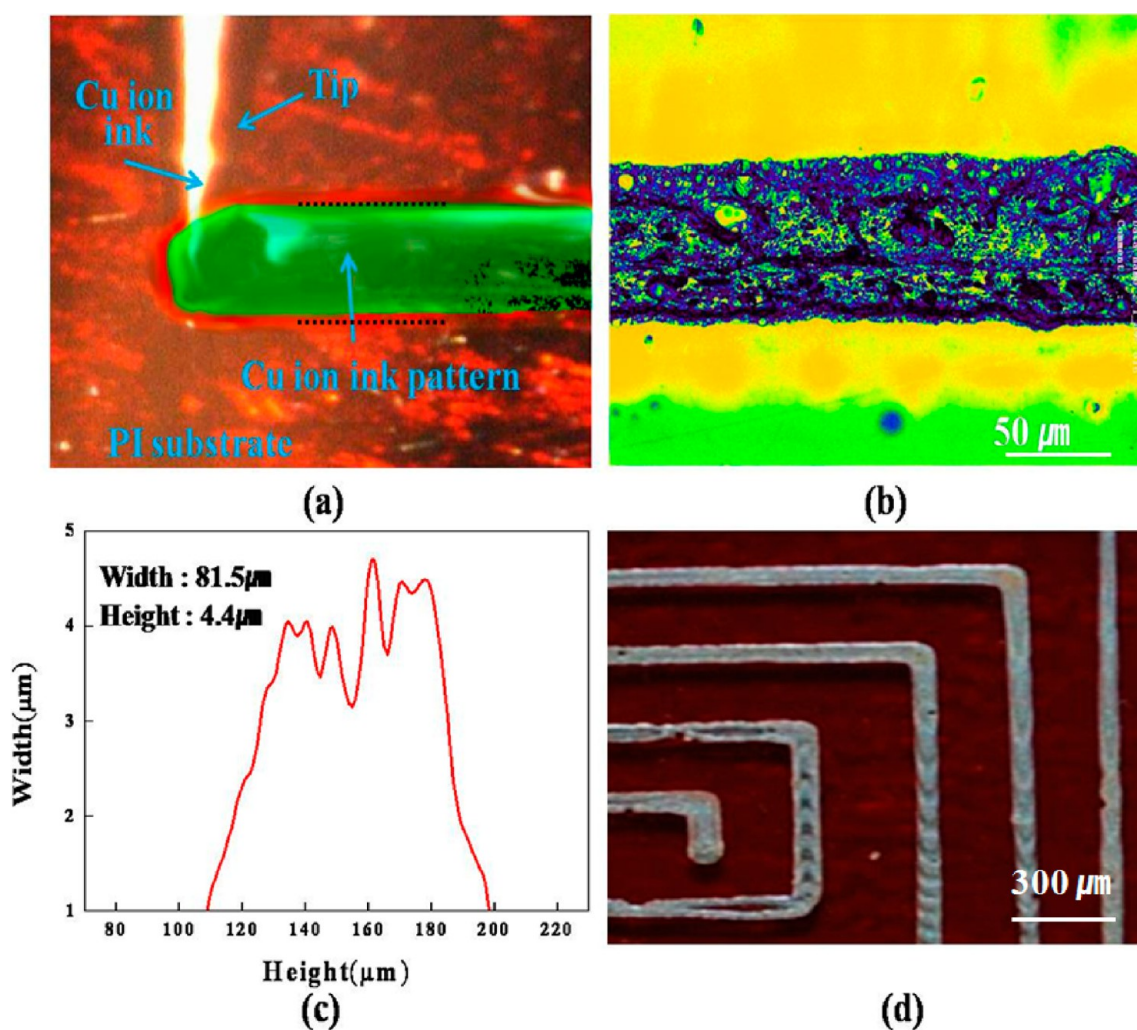


**Figure 7.** Fabrication of a microconductive line: (a) as-printed line using the SonoPlot GIX Desktop Microplotter, (b) 2D image of the microconductive line after IPL treatment, (c) surface profile of the conducting Cu electrode (Alpha-step IQ), and (d) spiral-type micropattern (line width: 81  $\mu\text{m}$ ).

ion ink could be fabricated. Moreover, the problem of restricted use of substrates due to the high sintering temperature of Cu was resolved by employing an IPL, which allows large-area, high-speed sintering at room temperature and normal atmospheric pressure. Regarding the high oxidization of the Cu nanoparticles, pure Cu films could be fabricated without the formation of oxide when using reducing gases with formic acid and ammonia upon light sintering.

The IPL treatment as a function of the pulsed light energy revealed that organic substances and other additives did not combust at 16–30.5  $\text{J cm}^{-2}$ ; therefore, complete sintering failed to occur upon a heat treatment, and the existence of  $\text{Cu}_2\text{O}$  was the cause of the high resistance. Moreover, excellent electrical properties at a resistivity level in the range of 3.21–5.27  $\mu\Omega\text{-cm}$  were found when the light energy ranged from 40 to 60  $\text{J cm}^{-2}$ , at which setting patterns of pure Cu phases could be fabricated.

This study establishes the conditions for the fabrication of Cu ion ink. As a result, micro- and homogeneous patterns with high electric conductivity can now be implemented instantly. Furthermore, it is anticipated that pen and inkjet printing processes will be used to reduce the overall costs, in terms of both time and space, leading to additional economic benefits. The findings of this study are expected to lead to innovative

and wide-ranging changes in various industries including electrics, electronics, semiconductors, automobiles, aerospace, and mechanics (precision parts).

## ■ ASSOCIATED CONTENT

### 📄 Supporting Information

Surface profiles of inkjet printing and roller ball pen printing; ILP characteristics; adhesion test results; additional optical and SEM images. This material is available free of charge via the Internet at <http://pubs.acs.org>.

## ■ AUTHOR INFORMATION

### Corresponding Author

\*E-mail: [youngjei@kist.re.kr](mailto:youngjei@kist.re.kr). Fax: +82-2-958-5554. Tel: +82-2-958-5553.

### Notes

The authors declare no competing financial interest.

## ■ REFERENCES

- (1) Perelaer, J.; Smith, P. J.; Mager, D.; Soltman, D.; Volkman, S. K.; Subramanian, V.; Korvink, J. G.; Schubert, U. S. *J. Mater. Chem* **2010**, *20*, 8446.

- (2) Berggren, M.; Nilsson, D.; Robinson, N. D. *Nat. Mater.* **2007**, *6*, 3–5.
- (3) Siringhaus, H.; Kawase, T.; Friend, R. H.; Shimoda, T.; Inbasekaran, M.; Wu, W.; Woo, E. P. *Science* **2000**, *290*, 2123–2126.
- (4) Perelaer, J.; Klokkenburg, M.; Hendriks, C. E.; Schubert, U. S. *Adv. Mater.* **2009**, *21*, 4830–4834.
- (5) Fisslthaler, E.; Sax, S.; Scherf, U.; Mauthner, G.; Moderegger, E.; Landfester, K.; List, E. J. W. *Appl. Phys. Lett.* **2008**, *92*, 183305.
- (6) Cao, Q.; Kim, H. S.; Pimparkar, N.; Kulkarni, J. P.; Wang, C.; Shim, M.; Roy, K.; Alam, M. A.; Rogers, J. A. *Nature* **2008**, *454*, 495–500.
- (7) Kim, Y. H.; Yoo, B. W.; Anthony, J. E.; Park, S. K. *Adv. Mater.* **2012**, *24*, 497–502.
- (8) Choi, Y. H.; Lee, J. H.; Kim, S. J.; Yeon, D. H.; Byun, Y. H. *J. Mater. Chem.* **2012**, *22*, 3624–3631.
- (9) Lim, J. A.; Lee, W. H.; Lee, H. S.; Lee, J. H.; Park, Y. D.; Cho, K. W. *Adv. Funct. Mater.* **2008**, *18*, 229–234.
- (10) Perelaer, J.; Abbel, R.; Wünscher, S.; Jani, R.; van Lammeren, T.; Schubert, U. S. *Adv. Mater.* **2012**, *24*, 2620–2625.
- (11) Lee, Y. I.; Lee, K. J.; Goo, Y. S.; Kim, N.; Byun, W. Y.; Kim, J.; Yoo, D. B.; Choa, Y. H. *Jpn. J. Appl. Phys.* **2010**, *49*, 086501.
- (12) Jo, Y. H.; Jung, I. Y.; Choi, C. S.; Kim, I. Y.; Lee, H. M. *Nanotechnology* **2011**, *22*, 225701.
- (13) Ko, S. H.; Pan, H.; Hwang, D. J.; Chung, J.; Ryu, S.; Grigoropoulos, C. P.; Poulidakos, D. *J. Appl. Phys.* **2007**, *102*, 093102.
- (14) Reinhold, I.; Hendriks, C. E.; Eckardt, R.; Kranenburg, J. M.; Perelaer, J.; Baumann, R. R.; Schubert, U. S. *J. Mater. Chem.* **2009**, *19*, 3384–3388.
- (15) Perelaer, J.; de Gans, B. J.; Schubert, U. S. *Adv. Mater.* **2006**, *18*, 2101–2104.
- (16) Ryu, J. G.; Kim, H. S.; Hahn, H. T. *J. Electron. Mater.* **2011**, *40*, 42–50.
- (17) Kim, H. S.; Dhage, R.; Shim, D. E.; Hahn, H. T. *Appl. Phys. A: Mater. Sci. Process.* **2009**, *97*, 791–798.
- (18) Han, W. S.; Hong, J. M.; Kim, H. S.; Song, Y. W. *Nanotechnology* **2011**, *22*, 395705.
- (19) Lee, D. J.; Park, S. H.; Jang, S.; Kim, H. S.; Oh, J. H.; Song, Y. W. *J. Micromech. Microeng.* **2011**, *21*, 125023.
- (20) Willix, R. L. S.; Garrison, W. M. *J. Phys. Chem.* **1965**, *69*, 1579–1583.
- (21) Zeng, D.; Cheng, J.; Ren, S.; Sun, J.; Zhong, H.; Xu, E.; Du, J.; Fang, Q. *React. Funct. Polym.* **2008**, *68*, 1715.
- (22) Park, S. I.; Ahn, J. H.; Feng, X.; Wang, S. d.; Huang, Y. G.; Rogers, J. A. *Adv. Funct. Mater.* **2008**, *18*, 2673–2684.
- (23) Choi, C. S.; Jo, Y. H.; Kim, M. G.; Lee, H. M. *Nanotechnology* **2012**, *23*, 065601.
- (24) Kim, I.; Kim, J. *J. Appl. Phys.* **2010**, *108*, 102807.
- (25) Lee, Y. I.; Lee, K. J.; Goo, Y. S.; Kim, N. W.; Byun, Y.; Kim, J. D.; Yoo, B.; Choa, Y. H. *Jpn. J. Appl. Phys.* **2010**, *49*, 086501.
- (26) Lee, Y. G.; Choi, J. R.; Lee, K. J.; Stott, N. E.; Kim, D. H. *Nanotechnology* **2008**, *19*, 415604.
- (27) Woo, K. H.; Kim, D. J.; Kim, J. S.; Lim, S. K.; Moon, J. H. *Langmuir* **2009**, *25*, 429–433.